Use of Multi-Source Data Sets for Land Use/Land Cover Classification in a Hilly Terrain for Landslide Study

D. P. Kanungo and S. Sarkar

Abstract

The land use/land cover (LULC) information of an area is essential for monitoring and management of natural resources. It is an important input for many geological, hydrological, ecological and agricultural models. In this study, the IRS-1C LISS-III data have been used as the primary data source along with NDVI (Normalized Difference Vegetation Index) and DEM (Digital Elevation Model) images as additional data layers to improve the LULC classification accuracy in a hilly terrain. Image classification is performed using most widely used Maximum Likelihood Classifier (MLC). The IRS-1C PAN image is used as the reference data for generating training and testing datasets. The preparation of reference data is ably supported with field data as well as information from topographic maps. The results show a reasonable improves in the accuracy of classification on incorporation of NDVI and DEM as ancillary data. The LULC map thus prepared is useful as one of the input data layers for landslide hazard study. High spatial resolution IRS-1CPAN and PAN-sharpened LISS-III images were used to prepare a landslide distribution map which was verified from field surveys. Landslide density is found to be maximum in barren lands, followed by agriculture land, built-up land, tea plantation area, and forest cover. The relation between LULC and landslide density thus obtained was later used as an input for landslide susceptibility mapping.

Key word: *Land use, Land cover, image classification, multi-source, landslide*

Geotechnical Engineering Division, CSIR-Central Building Research Institute,
Roorkee 247 667, India
debi.kanungo@gmail.com, shantanu_cbri@yahoo.co.in

Introduction

The land use/land cover (LULC) information of an area is essential for proper planning, management and monitoring of natural resources. It is an important input for many geological, hydrological, ecological and agricultural models. LULC map generally shows distribution of forest cover, water bodies and types of land use practices. Many studies (e.g., Coppin and Richards, 1990; Selby, 1993; Mehrotra *et al.*, 1996) have revealed a clear relationship between vegetation cover and slope instability.

Remote sensing images help in gathering quality LULC information at local, regional and global scales because of its synoptic view, map like format and repetitive coverage (Csaplovics, 1998; Foody, 2002). Further, in mountainous regions like the Himalayas, particularly in the inaccessible areas due to high altitudes and ruggedness in the terrain, remote sensing images are quite useful for mapping. Due to changes in topographical and environmental conditions, spectral characteristics also change from region to region (Arora and Mathur, 2001). Therefore, the approach for LULC classification that incorporates ancillary data from other sources may be more effective than that is based solely upon multi-spectral data from one sensor. The topographic maps are useful in generating the DEM, which along with its attributes, such as slope and aspect; provide the basis for multi-source classification (Strahler *et al.*, 1978; Jones *et al.*, 1988; Frank, 1988; Janssen *et al.*, 1990; Saha *et al.*, 2005). Furthermore, the derivatives of multispectral images like Principal Components Analysis (PCA) and Normalised Difference Vegetation Index (NDVI) may also be useful to improve the LULC classification from remote sensing data in mountainous regions (Eiumnoh and Shrestha, 2000; Saha *et al.*, 2005). In mountainous terrain, such as Himalayas, shadow is the major problem in achieving the accurate land use land cover classification from remote sensing data. The use of NDVI image as an additional layer for classification has been recommended to overcome this problem, since the band ratio derivatives may help in nullifying the topographic effect to some extent (Holben and Justice, 1981; Apan, 1997). However, NDVI alone may not be able to eliminate the shadow effect completely. Later, Eiumnoh and Shrestha (2000) and Saha *et al.* (2005) incorporated both NDVI and DEM images as additional layers in the classification process and found a significant improvement in the classification accuracy.

This study focuses on Darjeeling hill which lies between latitudes 26°56'N and 27°8'N and longitudes 88°10'E and 88°25'E and covers an area of about 254 km^2 (Figure 1). The main habitat areas are Darjeeling, Ghum, Sonada, and Sukhiapokhri. The maximum elevation of 2,584 m occurs at the Tiger hill. The area is dominated by slopes ranging between 15° and 35° while steep slopes (i.e., >35°) occupy a smaller area. The annual

rainfall in the region varies from a low of 3,000 mm to a high of 6,000 mm. The major land use practice in the study area is tea plantation and agriculture mostly developed around the habitat areas.

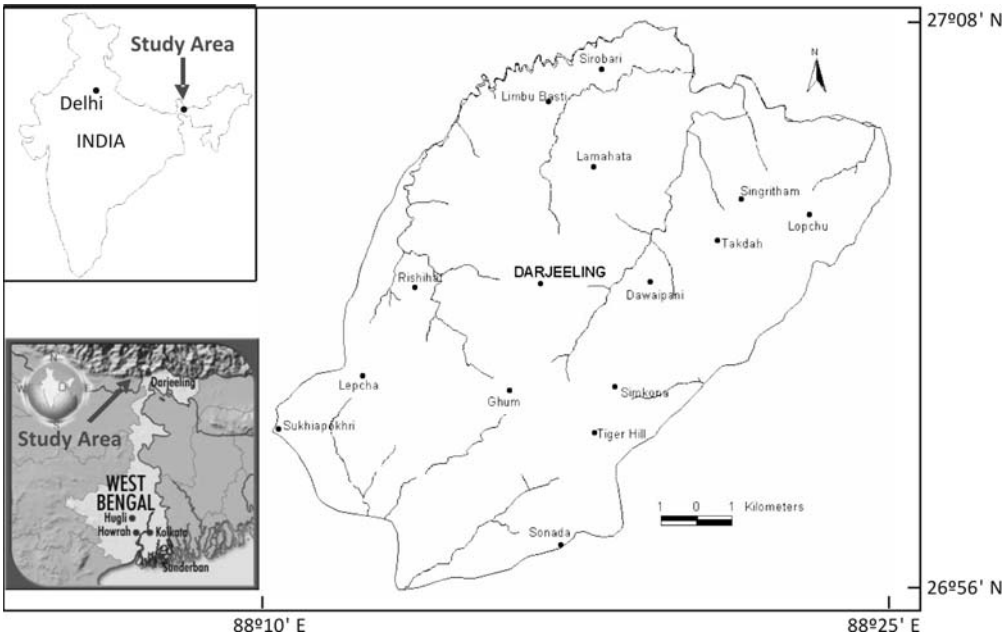

Fig 1. Study area

In this study, the IRS-1C LISS-III data (22nd March, 2000) with a spatial resolution of 23.5m has been used as the primary data source along with NDVI and DEM images as additional data layers to implement multi-source LULC classification process. A separability analysis using transformed divergence is performed to examine the significance of various spectral bands in the classification process. Most widely used Maximum Likelihood Classifier (MLC) is used to perform the classification. A very small portion covered by the cloud and its shadow in the original LISS-III image has been masked and then used as the primary data to perform LULC classification. The PAN image (3rd April, 2000) with a spatial resolution of 5.8m is used as the reference data for generating training and testing datasets. This is in accordance with other studies on LULC classification of remote sensing data, where finer resolution data have also been used as reference data (Fisher and Pathirana, 1990; Foody and Arora, 1996; Shalan *et al.*,

2003; Saha *et al.*, 2005). The preparation of reference data is ably supported with field data as well as information from topographic maps. The LULC map thus produced was used for landslide hazard study. High spatial resolution IRS-1C-PAN and PAN-sharpened LISS-III images were used to produce a landslide distribution map which was verified from field surveys. A total of 101 landslides showing areas occupied by sliding activity were identified. The landslide distribution in different categories of land use land cover in the area was also analyzed.

Methodology

A multi-source image classification involves a number of steps which include generation of ancillary data layers (NDVI and DEM), image classification and accuracy assessment.

Geometric registration of images

The digital images acquired from remote sensing satellites are fraught with geometric distortions, which render them unusable, as these may not be directly correlated to ground locations (Gupta, 2003). Geo-referencing involves the process of assigning map coordinate information to the image data so that the geometric integrity of the map in the image is achieved.

In this study, the geo-referencing of remote sensing data (IRS-1C LISS-III and IRS-1D PAN Images) has been performed using ERDAS Imagine software. In the first step, the Survey of India topographic maps have been geo-referenced to geographic coordinate system. These maps have been later used as reference maps for geo-referencing of satellite images.

The IRS-1C LISS-III image has been geo-referenced with the topographic maps by taking input GCPs from the LISS-III image and reference GCPs from topographic maps. A total of 35 well distributed GCPs have been considered for registration and an RMS control point error of 0.83 pixels is obtained. Also, the registration is checked with another set of independent 11 GCPs, which yielded an RMS error of 0.96. It is found that the RMS errors obtained using 1st order polynomial model for geometric correction is within the acceptable limit of one pixel. The nearest neighbor resampling method has been adopted to produce the geo-referenced LISS-III image (Figure 2), as this preserves the original brightness values in the output image.

Co-registration of IRS-1D PAN with IRS-1C LISS-III image is essential in view of the fact that the PAN image is used for selecting training and testing data samples for multispectral (LISS-III) image classification. Therefore, the PAN image has been registered with LISS-III image by taking input GCPs from the PAN image and reference

GCPs from LISS-III image. In this co-registration process, a set of 50 well distributed GCPs produced an RMS control point error of 0.71 pixels and 15 check GCPs yielded an RMS error of 0.68 pixels. The 1st order polynomial model with nearest-neighbor resampling method is used for this purpose. The registered PAN image thus obtained is shown in Figure 3.

The optical remote sensing images invariably contain the effect of selective atmospheric scattering and absorption of the solar radiation. In the visible - near infrared region of the electromagnetic spectrum, scattering is the most dominant process leading to path radiance. This has an additive role and affects the brightness values (Jensen, 1996). The remote sensing data, therefore, need to be corrected. Although, there are many techniques to perform this correction, the most widely used, the 'dark object subtraction' technique (Chavez, 1988) has been adopted to correct the atmospheric scattering. The minimum DN values for green, red, near infrared (NIR) and shortwave infrared (SWIR) bands were extracted and were expected to be due to path radiance. These values were subtracted from DN values of pixels in the respective bands to generate a path radiance corrected image. The corrected LISS-III and PAN images formed the data sources for preparation of land use land cover map.

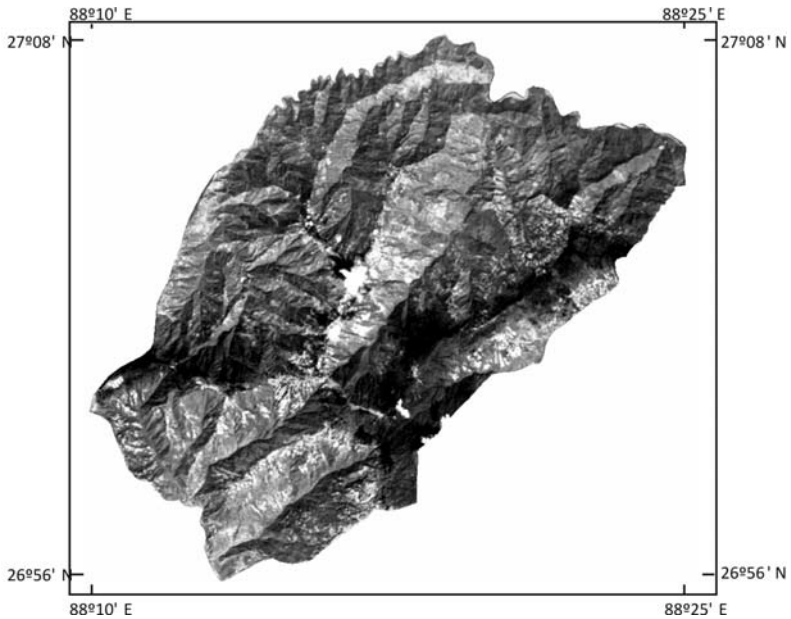

Fig 2. IRS-1C LISS-III False Colour Composite (NIR=R, Red=G, Green=B)

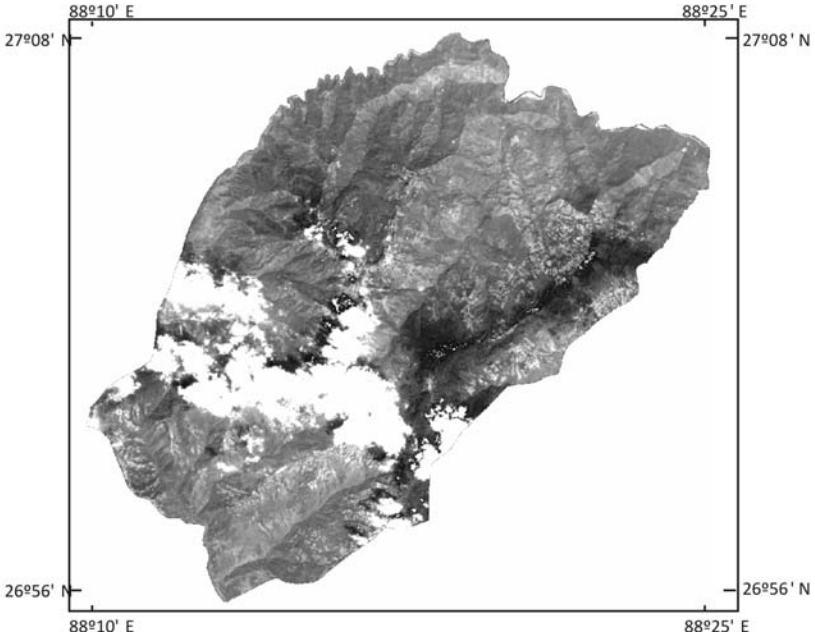

Fig 3. IRS-1D PAN image of the area (A large portion of this image is covered by clouds)

Ancillary Data generation

NDVI layer

During field surveys, different types of vegetation were observed in the study area. Hence, NDVI has been used as an ancillary data layer in the classification process to enhance the separability among various vegetation classes, and also to reduce the effect of shadow due to topography. The NDVI can be stated as,

$$NDVI = (NIR\ band - Red\ band) / (NIR\ band + Red\ band) \quad (1)$$

The DN values of pixels of the NDVI image thus produced range from 0.00 to 0.83 with higher values indicating increasing biomass. The positive values represent various types of vegetation classes. Near zero values indicate non-vegetation classes, such as water, river sand and barren land.

DEM layer

DEM represents the spatial variation of elevation over an area. It is an important basic

component in LSZ studies. In this study, DEM has been used as an input layer to multi-source classification of remote sensing data for land use land cover map preparation to minimize the error in classification due to topographic variations.

The DEM has been prepared using the conventional and most prevalent method by considering the contours from Survey of India topographic maps. The contours at 10m and 20m intervals on 1:25,000 scale topographic maps and 40m interval on 1:50,000 scale maps respectively have been used to generate the DEM using the triangulated irregular network (TIN) method. A DEM at spatial resolution corresponding to pixel size of 25m × 25m has been generated to match the nominal spatial resolution of LISS-III image.

Image Classification

Image classification process is based on several steps, a) selection of LULC classification scheme, b) formation of training dataset, c) separability analysis, d) Maximum Likelihood Classification (MLC) and e) accuracy assessment. The methodology of multi-source image classification for LULC is given in figure 4.

Selection of LULC classification scheme

A classification scheme defines the LULC classes to be considered to prepare land use land cover map from remote sensing image data. The number of LULC classes are sometimes chosen according to the requirements of the specific project for a particular application (Arora and Mathur, 2001; Saha *et al.*, 2005). In this study, the LULC classes are chosen keeping in view its application for landslide studies. During field visits, eight classes were identified in the study area. These classes are dense forest, sparse forest, tea plantation, agriculture, barren, built up, water bodies and river sand. Detailed description of all these classes along with their interpretative characteristics on the FCC of LISS-III image and PAN image is given in Table 1. This information is used to identify the training and testing areas on the image for carrying out supervised classification and accuracy assessment.

Formation of training dataset

The success of image classification highly depends on the quality of training dataset which in turn depends on the capability of image interpretation and knowledge on the LULC patterns of the study area. In this study, the number of training pixels for each class (Table 2) was defined in accordance with the proportion of the area covered by the respective classes on the ground. Similar to other studies, the fine spatial resolution PAN

image and Survey of India topographic maps were used as reference data for ground truths to demarcate the training pixels on the LISS-III image. All the eight LULC classes were visually interpreted on the PAN image based on their characteristics. The PAN image derived information and ground truth data from field survey were used to demarcate training areas on LISS-III image for all the classes. Majority of training areas were normally distributed, which is a basic requirement of the maximum likelihood classifier used in this study.

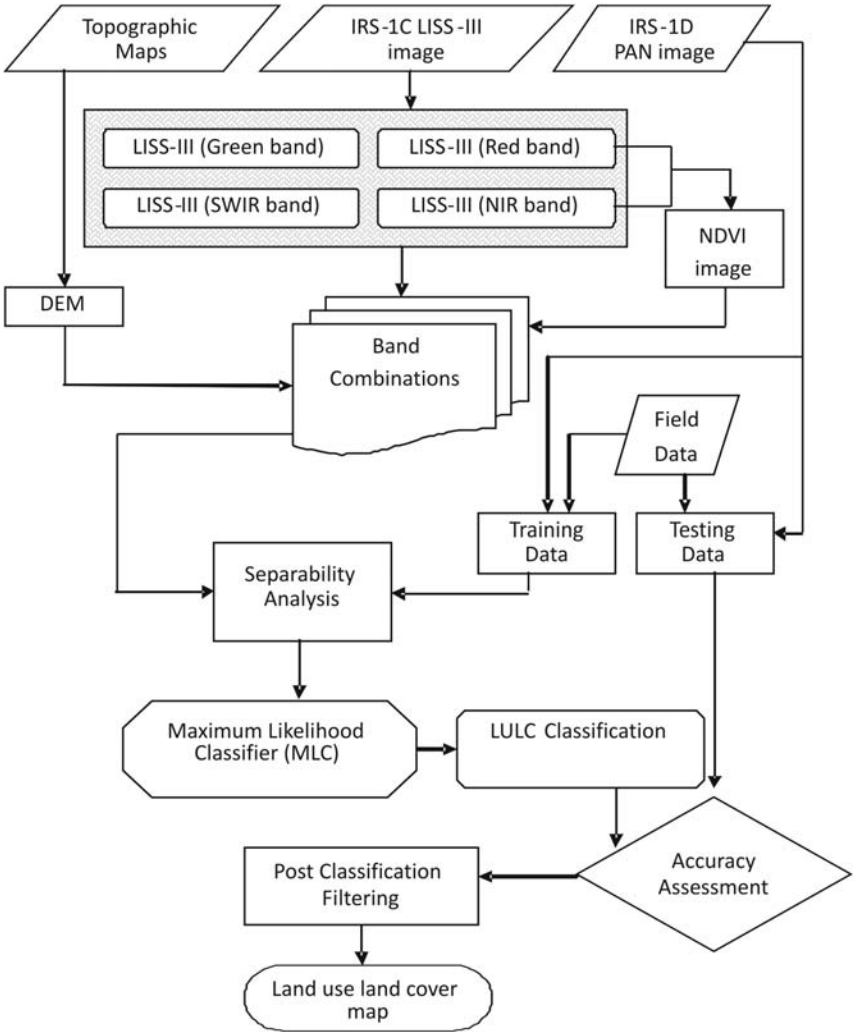

Fig 4. Methodology for multi-source LULC classification

Table 1. Characteristics of LULC classes

Land use land cover class	Description	Interpretation on LISS-III colour infrared composite	Interpretation on PAN image
Dense forest	Tall dense trees	Dark red with rough texture	Dark tone with rough texture
Sparse forest	Scanty tall trees and low vegetation density with exposed ground surface	Dull red to pinkish	Light tone with dark patches
Tea plantation	Tea plants with moderate vegetation density	Pink and smooth appearance	Light tone with smooth patches
Agriculture	Crops on hill terraces as step cultivation	Dull red and smooth appearance	Step like arrangement of fields and bright tone with smooth texture
Barren land	Exposed rocks/soils without vegetation	Yellowish	Very bright tone
Built up area	Towns and villages; block like appearance	Bluish	Typical blocky appearance with light tone
Water bodies	Rivers and lakes	Cyanish blue to blue according to the depth of water and sediment content	Dark tone
River sand	River sediments on the bank	Cyanish	Bright tone

Table 2. Number of training pixels for LULC classes used in image classification

Land use land cover class	Number of training pixels
Dense forest	1129
Sparse forest	622
Tea plantation	1127
Agriculture	639
Barren land	204
Built up area	288
Water bodies	193
River sand	273

Separability analysis

A separability analysis was performed with multi-source data layers using the training dataset of all the eight LULC classes to observe the spectral discrimination between these classes. In this study, a combination of six data layers comprising of Green, Red, Near Infrared (NIR) and Shortwave Infrared (SWIR) bands of multispectral LISS-III image, NDVI and DEM data layers were used as the input dataset for multi-source classification. Separability is a statistical measure devised on the basis of spectral distances computed for a combination of bands. From a number of separability measures, the Transformed Divergence (TD) measure (Janssen *et al.*, 1990) has been adopted in this study. The TD values range from 0 to 2000. A value close to 2000 indicates the best separability between the classes. The values between 1800 and 2000 are generally considered adequate to proceed for classification. As the present study intends for a multi-source classification, the average TD values of various band combinations including the ancillary data were computed. The band combinations with four bands of LISS-III image, NDVI and DEM resulted in the highest average TD value of 1977 as compared to those for the combination of only four spectral bands of LISS-III image and another combination of four spectral bands of LISS-III image and NDVI. The lowest TD value of 1723 is obtained for the signatures of barren land and agriculture. This is on expected lines as the agriculture lands without cultivation appear to be barren lands. Hence, a low separability between these two classes is observed. This analysis indicates that LISS III image together with NDVI and DEM has produced the best separability amongst various pairs of LULC classes. All the three combinations were used to perform LULC classification.

Maximum Likelihood Classification (MLC)

Over the years a number of classifiers have been developed and tested for remote sensing image classification. Each of these classifiers has its own merits and demerits in terms of efficiency and accuracy. The maximum likelihood classifier (MLC) was found to be the most accurate and most widely used for image classification, when the data distribution assumptions are met. The MLC is based on the decision rule that pixels of unknown class membership are allocated to those classes with which they have the highest likelihood of membership (Foody *et al.*, 1992). The details on this classifier may be found in Richards and Jia (1999). In this study, the MLC has been used to produce land use land cover maps, as it takes the variability of classes into account via covariance matrix.

Accuracy Assessment of LULC Classification

A testing dataset has been prepared with the help of reference data (PAN image and field data). The class allocation of each pixel in the classified image is compared with the corresponding class allocation on reference data to determine the classification accuracy. The pixels of agreement and disagreement are compiled in the form of an error matrix where the rows and columns represent the number of LULC classes and the elements of the matrix represent the number of pixels in the testing (reference) dataset. A number of accuracy measures, such as overall accuracy, user's accuracy and producer's accuracy can be estimated from the error matrix (Congalton, 1991). The overall accuracy indicates the accuracy of classification as a whole, where as user's and producer's accuracy measures indicate the accuracy of individual LULC classes.

In the present study, field data on LULC classes and finer resolution PAN image have been used as reference data to prepare testing dataset for accuracy assessment. The testing pixels for each class have been randomly selected. These pixels are distributed all over the study area and are larger than 75 to 100 pixels per class as recommended by Congalton (1991) for accuracy assessment purposes. For comparison, the same testing dataset was used to determine the overall and producer's accuracy from different LULC classifications.

Results and Discussions

The objective of this study is to perform a multi-source classification including spectral and ancillary data to produce an accurate LULC map for its use in landslide study.

LULC Classification

The overall classification accuracy of 91.7% has been obtained in case of the dataset

using a combination of four spectral bands of LISS III image, NDVI and DEM. The overall accuracy corresponding to other two combinations (four spectral bands of LISS III image; four spectral bands of LISS III image and NDVI) are 88.1% and 89.4% respectively. Hence, it is clearly observed that on inclusion of NDVI and DEM data layers with the spectral data of LISS III, the overall accuracy for LULC classification is increased.

The accuracy of individual LULC classes was assessed based on producer's accuracy for all the three combinations (Table. 3). A glance at producer's accuracy values shows that the accuracy of all the LULC classes has increased gradually when NDVI and DEM data layers are included one by one in the classification process. This highlights that the misclassifications between the classes have been reduced.

It is observed in case of 6 data layer combination (LISS III, NDVI & DEM) producing highest overall classification accuracy that all the individual LULC classes except barren lands, built-up areas and water bodies have shown more than 90% producer's accuracy. The class barren land has been misclassified to some extent with the agriculture and tea plantation classes whereas the class built-up area has been misclassified with the classes tea plantation, agriculture, barren land and sparse forest. The class water body has been considerably misclassified with the class river sand.

Table 3. Producer's accuracy of individual LULC classes derived from accuracy assessment of classifications using different combinations

LULC classes	Producer's accuracy (%)		
	LISS III (4 spectral bands)	LISS III + NDVI	LISS III + NDVI+DEM
Dense forest	98.5	98.3	98.6%
Sparse forest	93.5	94.8	97.2%
Tea plantation	96.6	98.3	99.2%
Agriculture	82.6	89.5	95.9%
Barren land	81.2	79.0	82.3%
Built-up area	75.4	76.7	78.1%
Water body	86.3	87.5	89.2%
River sand	90.4	91.5	93.4%

The LULC classified image with highest accuracy contained some stray pixels over the whole image. To generate a smooth image by removing these stray pixels, a 3 × 3 pixels majority filter has been applied which assigns the most dominant class to the central pixel. Subsequently, the LULC information of the masked portion in the original

LISS III image has been replaced by the information collected from the topographic maps and some field data. The land use land cover layer thus prepared is shown in Figure 5. It can be observed that the northeastern, southeastern and southwestern parts of the area are dominated by thick forests. Tea plantation and sparse forests are the major land use land cover categories, which are distributed all over the area. The area-wise distribution of different LULC categories has been derived and is listed in Table 4. It is observed that the most frequent categories of LULC are tea plantation and sparse forest, followed by thick forest, agriculture land, barren land, habitation, the least being water bodies and river sand.

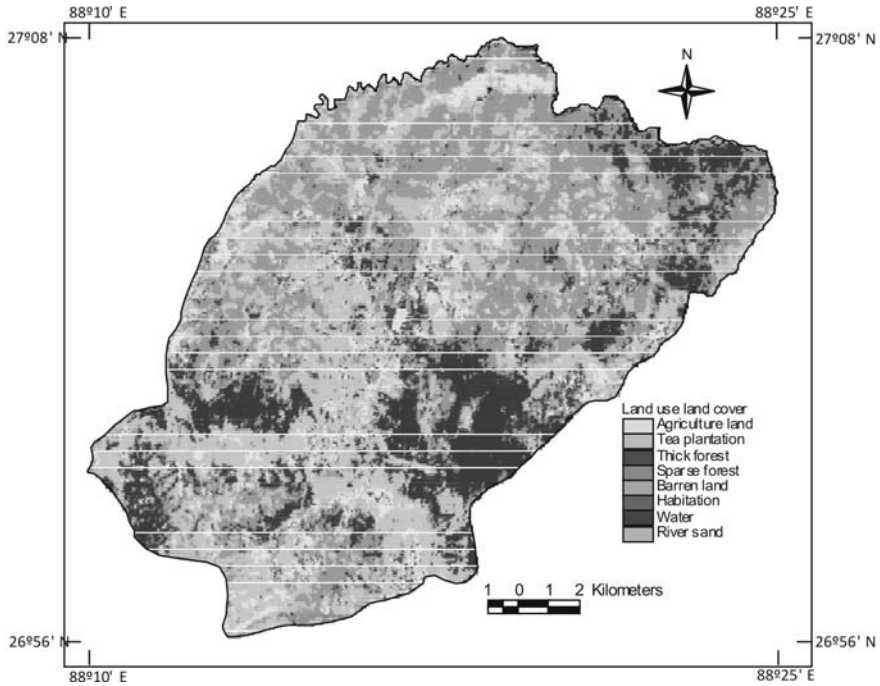

Fig 5. Land use/land cover map of the area

Landslide scenario in different LULC classes

Mapping of existing landslides is essential to understand the relationships between the landslide distribution and the causative factors, specifically land use land cover factor in this case. As, it is just not possible to map each and every landslide via field surveys in such a rugged terrain, a comprehensive mapping of landslide was undertaken through remote sensing image interpretation, aided by field verifications.

The identification of landslides on remote sensing image is based on the spectral characteristics, shape, contrast and the morphological expression. In general, there is a distinct spectral contrast between landslides and the background area. High spatial resolution IRS-1C-PAN and PAN-sharpened LISS-III images have been used for landslide identification, recognition and mapping. On the PAN image, landslides appear as features of very light tones due to rock debris without any vegetation on the slope. After enhancing the contrast of the PAN image, landslides occurring in barren areas could also be identified. A few old landslides were identified on the basis of their shape, landform and drainage. Feature extraction and interpretation is highly effective by using PAN-sharpened multi-spectral image products (Welch and Ehler, 1987; EOSAT, 1994; Sabins, 1996; Sharma *et al.*. 1996; Saraf, 2000; Prakash, *et al.*, 2001; Sanjeevi *et al.*, 2001; Shanmugam and Sanjeevi, 2001; Gupta, 2003). On the PAN-sharpened LISS-III image, the landslides appear as bright-white features (due to high reflectance) that are easily distinguished from other features. Further, landslides are also characterized by fan shape, sharp lines of break in topography and sometimes due to local drainage anomaly. Often, the toe part of the slide gives rise to a debris flow channel.

Many of the landslides identified on both PAN and PAN-sharpened LISS-III images have also been verified in the field. A total of 101 landslides of varying dimensions (180 m^2 to 27400 m^2) were identified from remote sensing images and field surveys. Majority of landslides have an area-wise extent of 500 m^2 - 2000 m^2. Most of the observed landslides are rock slides. However, in some cases, complex types of failure are also present.

The spatial distribution of landslides in different LULC categories has been obtained (Table 4). It is observed that barren land and agriculture categories have maximum landslide densities in comparison to other categories as should be the case and water bodies and river sand categories are devoid of landslides.

Table 4. Distribution of existing landslides in different LULC categories

LULC categories	Area of LULC categories (km2)	Percent area (%) (a)	Landslide area per category (km2)	Percent Landslide area per category (%) (b)	Landslide Density (b/a)
Agriculture	22.3	8.8	0.053	25.0	2.84
Tea Plantation	89.1	35.0	0.052	24.6	0.703
Dense Forest	45.4	17.8	0.024	11.3	0.635
Sparse Forest	81.1	31.9	0.041	19.3	0.605
Barren Land	8.9	3.5	0.036	17.0	4.857
Habitation	6.5	2.6	0.006	2.8	1.077
Water	0.6	0.2	0.000	0.0	0.000
River Sand	0.6	0.2	0.000	0.0	0.000

Conclusions

In hilly regions like the Himalayas, particularly in the inaccessible areas due to high altitudes and ruggedness in the terrain, remote sensing images are the only available source for land use land cover mapping and monitoring. The factors influencing classification accuracy of various LULC classes in hilly areas using remote sensing data may be attributed to the presence of cloud cover, shadow, steep slopes, low sun angle and differential vegetation cover. Therefore, the approach for land use land cover classification that incorporates ancillary data from other sources has been more effective than that is based solely upon multi-spectral data from one sensor. The present study showed a reasonable improve in accuracy of LULC classification on incorporation of DEM and NDVI layers with IRS-LISS-III image. An overall classification accuracy of 91.7% and producer's accuracies for the majority of LULC classes of the order of above 90% were obtained in this case. It is also observed that the use of DEM and NDVI layers in the classification process could address the problem of misclassifications incurred due to the effect of shadow in the image and also due to the similarity in spectral characteristics of some classes such as barren lands and built-up areas in hilly regions. Hence, this study highlights the efficacy of multi-source classification to increase the accuracy of LULC classification in hilly regions like the Himalayas. However, the availability of multi-season LISS-III images would have probably provided better results.

Further, the spatial distribution of landslides in different LULC categories showed

that barren lands have the maximum landslide density, followed by agriculture land, built-up land, tea plantation area and forest cover. These results reflect the real field conditions in hilly terrains. The relationship thus obtained was later used as an input for landslide susceptibility mapping.

Acknowledgement

The authors are thankful to the Director, CSIR-Central Building Research Institute, Roorkee for granting permission to publish this paper. We are also thankful to the reviewers whose comments and suggestions helped to improve the quality of this paper.

References

1. Apan, A. A., (1997) Land Cover Mapping for Tropical Forest Rehabilitation Planning using Remotely-Sensed Data, *International Journal of Remote Sensing*, 18(5), 1029-1049.
2. Arora, M.K. and Mathur, S., (2001) Multi-source Classification using Artificial Neural Network in a Rugged Terrain, *GeoCarto International*, 16(3), 37-44.
3. Chavez, P. S. Jr., (1988) An Improved Dark Object Subtraction Technique for Atmospheric Correction of Multispectral Data, *Remote Sensing of Environment*, 24, 459-479.
4. Congalton, R. G., (1991) A review of assessing the accuracy of classifications of remotely sensed data, *Remote Sensing & Environment*, 37, 35-46.
5. Coppin, N. and Richards, I., (1990) Use of Vegetation in Civil Engineering. *Butterworths*, London.
6. Csaplovics, E., (1998) High Resolution Space Imagery for Regional Environmental Monitoring - Status quo and Future Trends, *International Archives of Photogrammetry and Remote Sensing*, 32(7), 211-216.
7. Eiumnoh, A. and Shrestha, P., (2000) Application of DEM Data to Landsat Image Classification: Evaluation in a Tropical Wet-Dry Landscape of Thailand, *Photogrammetric Engineering & Remote Sensing*, 66(3), 297-304.
8. EOSAT, (1994) Merge Process Enhances Value of Data Sets, *EOSAT Notes*, 9, 5.
9. Fisher, P. F. and Pathirana, S., (1990) The Evaluation of Fuzzy Membership of Land Cover Classes in the Suburban Zone, *Remote Sensing of Environment*, 34(2), 121-132.
10. Foody, G. M., (2002) Status of Land Cover Classification Accuracy Assessment, *Remote Sensing of Environment*, 80, 185-201.
11. Foody, G. M. and Arora, M. K., (1996) Incorporating Mixed Pixels in the Training, Allocation and Testing Stages of Supervised Classifications, *Pattern Recognition Letters*, 17, 1389-1398.
12. Foody, G. M., Campbell, N. A., Trodd, N. M. and Wood, T. F., (1992) Derivation and Applications of Probabilistic Measures of Class Membership from Maximum Likelihood Classification, *Photogrammetric Engineering & Remote Sensing*, 58, 1335-1341.
13. Frank, T. D., (1988) Mapping Dominant Vegetation Communities in the Colorado Rocky Mountain Front Range with LANDSAT Thematic Mapper and Digital Terrain Data, *Photogrammetric Engineering & Remote Sensing*, 54(12), 1727-1734.
14. Gupta, R.P., (2003) Remote Sensing Geology, 2nd Edition, *Springer-Verlag*, Berlin Heidelberg , Germany, 655p.
15. Holben, B. and Justice, C., (1981) An Examination of Spectral Band Ratioing to Reduce the Topographic Effect on Remotely Sensed Data, *International Journal of Remote Sensing*, 2(2), 115-133.
16. Janssen, L. F., Jaarsma, J. and Linder, E. van der., (1990) Integrating Topographic Data with Remote Sensing for Land-Cover Classification, *Photogrammetric Engineering & Remote Sensing*, 48(1), 123-130.
17. Jensen, J. R., (1996) Introductory Digital Image Processing: A Remote Sensing Perspective, 2nd Edition, *Prentice-Hall*, New Jersey, US, 318p.
18. Jones, A. R., Settle, J. J. and Wyatt, B. K., (1988) Use of Digital Terrain Data in the Interpretation of SPOT-1 HRV Multispectral Imagery, *International Journal of Remote Sensing*, 9(4), 669-682.
19. Mehrotra, G. S., Sarkar, S., Kanungo, D. P., Mahadevaiah, K., (1996) Terrain Analysis and Spatial Assessment of Landslide Hazards in parts of Sikkim Himalaya, *Geological Society of India*, 47, 491-498.
20. Prakash, A., Fielding, E. J., Gens, R., Genderen, J. L. van and Evans, D. L., (2001) Data Fusion for Investigating Land Subsidence and Coalfire Hazards in a Coal Mining Area, *International Journal of Remote Sensing*, 22(6), 921-932.
21. Richards, J. A. and Jia, X., (1999) Remote Sensing Digital Image Analysis: An Introduction, 3rd Edition, *Springer-Verlag*, Heidelberg, Germany, 363p.
22. Sabins, F. F., (1996) Remote Sensing Principles and Interpretations, *W. H. Freeman & Co.*, New York, US, 494p.
23. Saha, A. K., Arora, M. K., Csaplovics, E. and Gupta, R. P., (2005) Land Cover Classification Using IRS LISS III Image and DEM in a Rugged Terrain: A Case Study in Himalayas, *Geocarto International*, 20(2), 33-40.
24. Sanjeevi, S., Vani, K. and Lakshmi, K., (2001) Comparison of Conventional and Wavelet Transform Techniques for Fusion of IRS-1C LISS-III and PAN Images. In: Proceedings of ACRS 2001 - 22nd Asian Conference on Remote Sensing, 5-9 November, Singapore, 1, 140-145.
25. Saraf, A. K., (2000) IRS-1C-PAN Depicts Chamoli Earthquake Induced Landslides in Garhwal Himalayas, India, *International Journal of Remote Sensing*, 21(12), 2345-2352.
26. Selby, M., (1993) Hillslope Materials and Processes. *Oxford University Press*, Oxford.
27. Shalan, M. A., Arora, M. K. and Ghosh, S. K., (2003) An Evaluation of Fuzzy Classifications from IRS 1C LISS III Imagery: a Case Study, *International Journal of Remote Sensing*, 24(15), 3179-3186.
28. Shanmugam, P. and Sanjeevi, S., (2001) Analysis and Evaluation of Fusion Techniques using IRS-1C LISS-3 and PAN Data for Monitoring

Coastal Wetlands of Vedaranniyam, Tamil Nadu. In: *Proceedings of the National Symposium on Advances in Remote Sensing Technology with special emphasis on High Resolution Imagery & Annual Convention of Indian Society of Remote Sensing (ISRS)*, 11-13 December, Ahmedabad, India.

29. Sharma, P. K., Chopra, R., Verma, V. K. And Thomas, A., (1996) Flood Management using Remote Sensing Technology: The Punjab (India) Experience, *International Journal of Remote Sensing*, 17(17), 3511-3521.
30. Strahler, A. H., Logan, T. L. And Bryant, N. A., (1978) Improving Forest Cover Classification Accuracy from Landsat by Incorporating Topographic Information. In: *Proceedings of 12th Symposium Remote Sensing Environment*, Ann Arbor, Michigan, US, 2, 927-942.
31. Welch, R. and Ehlers, M., (1987) Merging Multi resolution SPOT HRV and Landsat TM Data, *Photogrammetric Engineering & Remote Sensing*, 53(3), 301-303.